Solid State Communications 197 (2014) 20–24

Contents lists available at ScienceDirect

Solid State Communications

journal homepage: www.elsevier.com/locate/ssc

Field-effect-induced two-dimensional electron gas utilizing modulation-doped ohmic contacts

Sumit Mondal [a,b], Geoffrey C. Gardner [a,c], John D. Watson [a,b], Saeed Fallahi [a,b], Amir Yacoby [e], Michael J. Manfra [a,b,c,d,*]

[a] Birck Nanotechnology Center, Purdue University, West Lafayette, IN 47907, United States
[b] Department of Physics and Astronomy, Purdue University, West Lafayette, IN 47907, United States
[c] School of Materials Engineering, Purdue University, West Lafayette, IN 47907, United States
[d] School of Electrical and Computer Engineering, Purdue University, West Lafayette, IN 47907, United States
[e] Department of Physics, Harvard University, Cambridge, MA 02138, United States

ARTICLE INFO

Article history:
Received 7 August 2014
Accepted 12 August 2014
by A. Pinczuk
Available online 20 August 2014

Keywords:
A: Semiconductors
B: Epitaxy
D: Electron transport

ABSTRACT

Modulation-doped AlGaAs/GaAs heterostructures are utilized extensively in the study of quantum transport in nanostructures, but charge fluctuations associated with remote ionized dopants often produce deleterious effects. Electric field-induced carrier systems offer an attractive alternative if certain challenges can be overcome. We demonstrate a field-effect transistor in which the active channel is locally devoid of modulation-doping, but silicon dopant atoms are retained in the ohmic contact region to facilitate reliable low-resistance contacts. A high quality two-dimensional electron gas is induced by a field-effect and is tunable over a wide range of density. Device design, fabrication, and low temperature (T=0.3 K) transport data are reported.

Nanostructures such as quantum point contacts and quantum dots fabricated on modulation-doped AlGaAs/GaAs heterostructures are widely used to explore nanoscale electron transport and are utilized extensively in spin-based approaches to quantum computing [1–8]. Modulation-doped GaAs/AlGaAs heterostructures possess several desirable attributes including very high mobility of the underlying two-dimensional electron gas (2DEG) and the relative ease of nanostructure fabrication. However, time-dependent fluctuations of the charge state of ionized dopants inherent to modulation-doping can have adverse effects on the behavior of nanostructures, and are a possible source of decoherence for spin-qubits [9,10]. Ionized dopants can act as active trapping sites for electrons injected from the metal surface gate through the Schottky barrier [11], giving rise to random switching of the charge state of the impurities. These fluctuations cause instability through a time-dependent potential landscape [10–13]. Methods such as 'bias cooling' in which nanostructures are cooled while a positive bias applied to the gates aid in reducing random telegraph noise [11], but charge noise is still believed to a dominant mechanism limiting gate fidelities in spin qubits [9].

Field-effect-induced 2DEG transistors (FETs) in GaAs/AlGaAs heterostructures have been investigated extensively [14–27] and might find utility as a platform to investigate spin-qubits in a low-noise environment if certain limitations can be overcome. The most widely studied device is the heterostructure-insulated-gate field-effect transistor (HIGFET), in which a highly-conducting n+ GaAs gate is grown on top of an insulating $Al_xGa_{1-x}As$ barrier layer by molecular beam epitaxy (MBE) [14–16,18,22]. HIGFET fabrication requires placing ohmic contacts in intimate contact with the primary AlGaAs/GaAs interface where the 2DEG will reside without shorting the ohmic contact to the n+ GaAs gate [17,18]. This challenging task becomes increasingly difficult for shallow 2DEG structures required for many nanostructure devices [15]. Device yield is often low and the devices can suffer from high contact resistance. Another FET design reported in the literature utilizes a lithographically-defined global top-gate deposited on top of insulators such as polyimides [17,19–20,23], nitrides [24,25] or oxides [26] separating the ohmic contacts from the gate. In this configuration the global top-gate must extend over the ohmic contact pad to ensure a continuous 2DEG to the ohmic contact. Progress has been made in creating a 2DEG on shallow undoped structures by this method [20,21] and the induced 2DEG can have high mobility [24,25] in deeper structures. Nevertheless, the requirement that the gate electrode overlaps the rough annealed ohmic metal enhances the possibility of undesired leakage paths [27,28].

* Corresponding author.
E-mail address: mmanfra@purdue.edu (M.J. Manfra).

http://dx.doi.org/10.1016/j.ssc.2014.08.011
0038-1098/

In general, the absence of dopants makes fabrication of reliable ohmic contacts with high yield and low contact resistance challenging [20,28] in completely undoped structures.

In this letter we demonstrate an alternative FET device design that is simple to fabricate, has reliable ohmic contacts and negligible gate leakage. The FET is devoid of the dopant atoms in the active channel but retains silicon doping in the region near the ohmic contacts reliably yielding low contact resistance. An AlAs etch-stop layer designed into the epilayer facilitates removal of the modulation-doping layer in specific locations by selective wet etching. The density of the field-induced 2DEG can be modulated from 6.5×10^{10} cm^{-2} to 2.7×10^{11} cm^{-2} and the 2DEG exhibits a maximum mobility of 2.4×10^{6} cm^2/Vs at $T=0.3$ K. The observation of extremely low hysteresis of the 2DEG density and mobility during multiple gate voltage sweeps and multiple thermal cycles indicates that this device design will yield stable nanostructures and provide a new platform to investigate spin qubits.

The underlying heterostructure of this device is grown by MBE. The 2DEG resides at a single GaAs/$Al_{0.26}Ga_{0.74}As$ heterojunction. Fig. 1(a) and (b) respectively, represents the schematic cross-section and the simulated bandstructure for the as-grown wafer. The heterostructure consists of a 1 μm thick GaAs channel grown on a (100) GaAs substrate followed by a 175 nm thick $Al_{0.26}Ga_{0.74}As$ barrier and a 10 nm GaAs cap. It is delta-doped with silicon to 1.85×10^{12} cm^{-2} at a setback of 75 nm above the primary GaAs/$Al_{0.26}Ga_{0.74}As$ interface. The salient feature of this structure is the presence of a 3 nm AlAs etch stop layer situated 10 nm below the doping layer. In the as-grown wafer the modulation-doped silicon layer results in the formation of a uniform 2DEG as shown in Fig. 1(b). However, the presence of the AlAs etch stop allows for the removal of the silicon doping layer, and hence the 2DEG, in specific sites defined by lithography. For the devices discussed here, a simple Hall bar geometry is employed.

Device fabrication proceeded as follows. 10 Small mesas were defined with standard photolithography. 5 of these mesas are shown in Fig. 1(d) which represents one-half of a full device. These mesas serve as the ohmic contacts and access connections to the field-induced 2DEG. After a dip in dilute buffered-oxide-etch (BOE) to desorb the surface oxide, the patterned chip was etched using a 6:1 citric acid: H_2O_2 mixture. The entire chip was etched past the Si doping layer to the AlAs etch stop, except for the 10 small mesas. The etch rate of the citric acid: H_2O_2 mixture was extremely sensitive to x, the mole fraction of $Al_xGa_{1-x}As$ [29]. The citric acid: H_2O_2 mixture etched the $x=0.26$ barrier at ~4.5 nm/s but stopped at the pure AlAs etch-stop immediately below dopant layer. Dilute BOE, which is highly selective in etching AlGaAs with mole fraction above $x=0.4$, was used to remove the sacrificial 3 nm AlAs layer. In the etched field that forms the conducting channel of our device, only the undoped 62 nm $Al_{0.26}Ga_{0.74}As$ barrier remains above the GaAs buffer. The contact mesas and the etched field were carefully investigated using atomic force microscopy for any defects or non-uniformity of surface morphology. Sub-nanometer surface roughness in the etched field was achieved. Ni/Ge/Au (30 nm/60 nm/120 nm) contacts were evaporated on part of the mesa regions and subsequently annealed at 440^{0}C for 2 minutes in a forming gas atmosphere to diffuse the alloy into the 2DEG. A 63 nm silicon nitride (Si_3N_4) gate insulator was then deposited at 300 °C utilizing a multistep deposition process to prohibit the upward propagation of pinhole defects. The final fabrication step was the deposition of the Ti/Au (15 nm/160 nm) gate over the insulating Si_3N_4 layer. Fig. 1(c) and (d) shows a schematic cross-section of the device design and the schematic top-view of the Hall-bar FET. It is important to note that the gate does not overlap the ohmic metal layer. This can be clearly seen in the optical micrograph of our completed device (Fig. 1(e)). This separation eliminates a potential leakage path between the gate and the annealed ohmic contact. The small region between the annealed

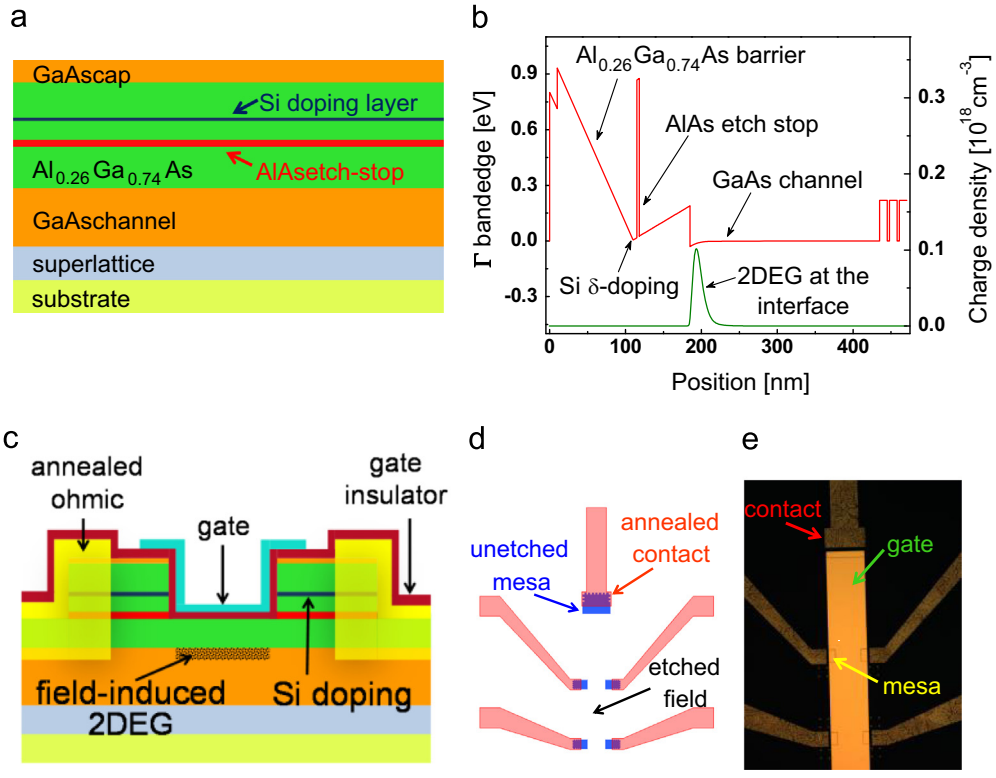

Fig. 1. (Color online) (a) Schematic cross-section of the MBE-grown wafer, (b) simulated bandstructure of the as-grown heterostructure using Nextnano3 [33], (c) schematic cross-section of the device design, (d) schematic top-view of a portion the FET, the top-gate is not shown for clarity, and (e) optical micrograph of the fabricated FET.

ohmic and the active field-effected 2DEG retains its modulation-doping and provides a low resistance path.

The completed FET was cooled to low temperature to characterize device operation, contact resistance, and magnetotransport quality. All of the measurements reported here were performed without illumination at the base temperature (T=0.3 K) of a Janis top-loading He^3 system using standard AC lock-in techniques at a frequency of 13 Hz with a 500 nA excitation current. Consistent with the operating principle of an enhancement-mode AlGaAs/GaAs FET, no conduction was observed in the device until the gate was biased above a threshold voltage necessary to place the conduction band minimum at the principal AlGaAs/GaAs interface below the Fermi level. The onset of conduction was observed in this particular device at a gate bias of 0.95 V. The bias voltage required to observe homogeneous transport in our devices varies from 0.75 V to 0.95 V. Below this threshold bias, a homogeneous density 2DEG is not formed. This threshold voltage for conduction is consistent with the Fermi level being pinned approximately 0.8 V below the GaAs conduction band at the Si_3N_4/GaAs interface. The GaAs/AlGaAs heterojunction was populated with an increasing density of carriers coming from the ohmic contacts as the gate was biased gradually beyond 0.9 V. The density was determined from the position of integer quantum Hall minima in the longitudinal resistance (R_{xx}). The density increased linearly with increasing gate bias and could be tuned from $\sim 6.5\times10^{10}\,\mathrm{cm}^{-2}$ to $\sim 2.6\times10^{11}\,\mathrm{cm}^{-2}$ with capacitance per area $3\times10^{11}\,\mathrm{cm}^{-2}$/V at T=0.3 K (Fig. 2(a)). This behavior indicated strong capacitive control of the 2DEG. The gate leakage was at or below 15 pA for all applied biases, the measurement noise-floor of this experiment. We note that the 2DEG density increases linearly up to gate bias 1.7 V. Above this point, the 2DEG density increase becomes sub-linear even though the gate leakage does not increase appreciably. This suggests that charge is accumulated at a secondary interface, most likely the Si_3N_4/AlGaAs interface. We only report transport in the linear regime between 0.95 V and 1.7 V.

The variation of the mobility of the FET with the 2DEG density is shown in Fig. 2(b). It rose from $4\times10^5\,\mathrm{cm}^2$/Vs at the onset of conduction to $2.4\times10^6\,\mathrm{cm}^2$/Vs, monotonically increasing with density. The highest mobility was comparable to the measured mobility of the underlying modulation-doped structure prior to any processing ($2.6\times10^6\,\mathrm{cm}^2$/Vs at T=0.3 K) indicating minimal processing related degradations. Insight into the dominant scattering mechanisms occurring in the channel can be obtained through examination of the density dependence of the mobility. The mobility (μ) was found to vary with density (n) as $\mu \propto n^{\alpha}$ with the exponent $\alpha = 1.03 \pm 0.02$. This value of α is interesting as it is intermediate between the value expected if the mobility-limiting scattering were dominated by uniformly distributed background charged impurities ($\alpha\sim0.7$) or dominated by remote ionized impurities ($\alpha\sim1.5$) typically associated with modulation doping [30,34]. Noting that there are no modulation-doped silicon atoms in the field-effected region, this behavior is somewhat unexpected. α=1.0 indicates that mobility is determined not only by uniformly distributed background impurities, but also by remote charged scattering sites, presumably at the Si_3N_4/AlGaAs interface that is only 62 nm away from the 2DEG in our device. We note that this observation is consistent with a recent prediction that the mobility in undoped devices will be impacted by surface scattering for a surface charge density of $1\times10^{11}\,\mathrm{cm}^{-2}$ once the surface comes within 60 nm of the 2DEG [36]. To further amplify our discussion of the dominant scattering mechanisms in our devices we present a comparison between the transport lifetime (τ_t) calculated from the mobility as $\tau_t = \mu m^*/e$ where m^* is the effective mass in GaAs and e is the charge of an electron and the quantum lifetime τ_q calculated from analysis of the low-field Shubnikov-de Haas oscillations through the relationship:

$$\Delta R_{xx} = 4R_0X(T)\exp-\left(\frac{\pi}{\omega_c\tau_q}\right)$$

where R_0 is the zero-field resistance, ω_c is the cyclotron frequency, and $X(T)$ is the thermal damping factor given by $X(T) = ((2\pi^2kT)/\hbar\omega_c)/\sinh((2\pi^2kT)/\hbar\omega_c)$. The transport lifetime τ_t is most sensitive to large-angle scattering while the quantum lifetime τ_q reflects both small-angle and large-angle scattering. Note that the transport lifetime shows a stronger dependence on 2DEG density than the quantum scattering time. This behavior is typically seen in high mobility GaAs structures [36]. The large ratio (10–30) between τ_t and τ_q is consistent with scattering dominated by long-range Coulomb scattering [37]. The ratio would be unity in the limit of short-range isotropic scattering. The behavior of the quantum lifetime further highlights that scattering in our device is controlled by charged impurities, located both at semiconductor/dielectric interface and uniformly distributed throughout the epitaxial layers (Fig. 3).

Fig. 4(a) displays transport in the quantum Hall regime at a gate voltage of 1.1 V. The high quality of the field-induced 2DEG is manifested in vanishing longitudinal resistance R_{xx} concomitant with plateaus in R_{xy}, corresponding to fully developed integer quantum Hall states. This data also confirmed the absence of any parallel conducting channel in the device. Reproducibility of the device is documented in Fig. 4(b). The 2DEG density was increased by ramping the gate from 0.95 V to 1.65 V (marked by the open blue squares in Fig. 4(b)) and then the gate potential was decreased which resulted in a non-hysteretic, highly repeatable, reduction in density as indicated by representative closed red stars in Fig. 4(b). Similar repeatability was observed for the mobility as indicated by the green squares and magenta triangles in the inset to Fig. 4(b). This behavior indicates minimal gate-induced

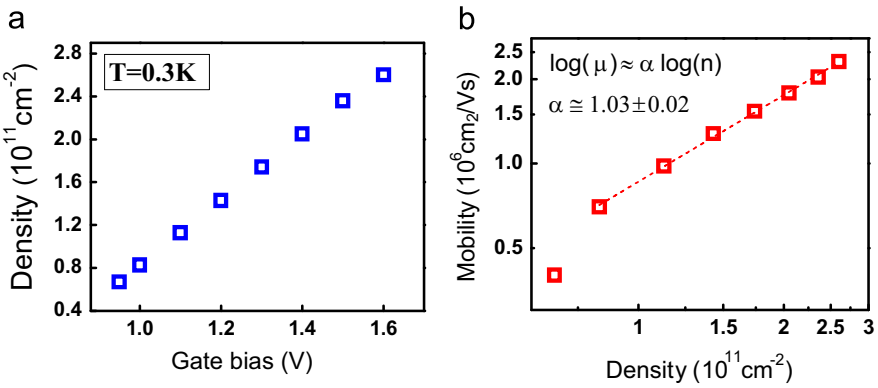

Fig. 2. (Color online) (a) Gate voltage dependence of the 2DEG density of the FET, and (b) density dependence of the 2DEG mobility of the FET on a log-log scale.

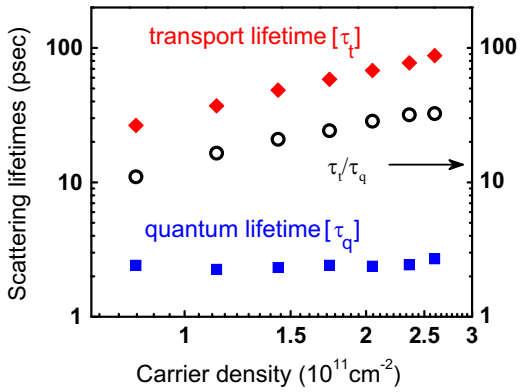

Fig. 3. (Color online) Transport lifetime (τ_t) derived from mobility measurements and quantum lifetime (τ_q) derived from Shubnikov de Haas oscillations in the FET as a function of density. The large ratio of τ_t/τ_q indicates the dominance of long-range Coulomb scattering.

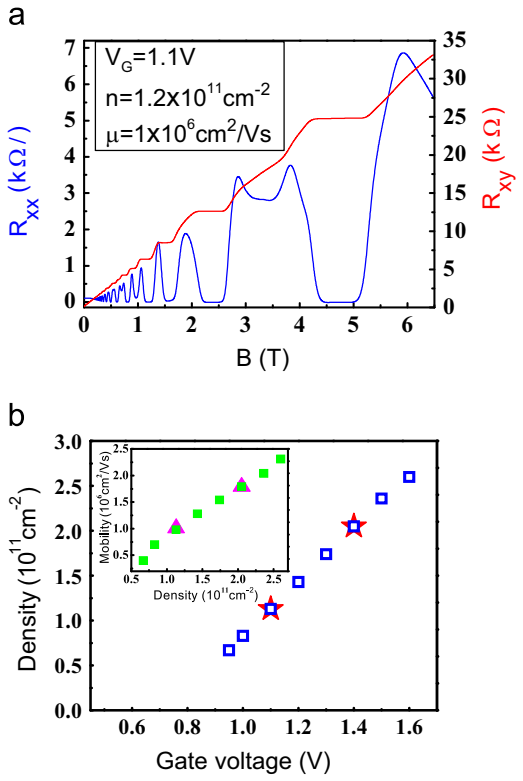

Fig. 4. (Color online) (a) Magnetotransport of the FET at a density 1.2×10^{11} cm^{-2}, and (b) stability of the device under gate operation. The open blue squares and the red stars show the measured density as the gate voltage is swept back and forth. In the inset the equivalent plot for mobility as a function of density is shown. The green squares and red triangles demonstrate the reproducibility of the mobility as the gate voltage is swept.

rearrangement of charge at the semiconductor-insulator interface. In addition, the low temperature electrical properties of the device were found to be completely reproducible over the course of several thermal cycles to room temperature. The contact resistance of the device was measured using a three-terminal method described in Ref. [32]. The measured contact resistance was $\sim$70 Ω. Since the gate does not overlap the ohmic metal in the device, the measured contact resistance is a sum of contributions from the annealed metal contact as well as the portion of mesa that extends from the ohmic metal to the gated region of the device. We note that low contact resistance ($R_c \leq 100\,\Omega$) is typically a necessary condition for high speed readout of spin qubits, as parasitic RC time constants can limit measurement bandwidth [35].

In conclusion, we have experimentally demonstrated the fabrication and operation of a FET device that utilizes modulation doping for reliable ohmic contact formation, but removes the dopant atoms in the active channel. The fabrication is relatively simple and high-yield. The resulting 2DEG has high mobility and is widely tunable in density from $\sim6.5\times10^{10}$ cm^{-2} to 2.6×10^{11} cm^{-2} with peak mobility 2.4×10^6 cm^2/Vs. The device is non-hysteretic, reproducible upon thermal recycling, and has minimal gate leakage. While a simple Hall bar geometry was explored here, this architecture is amenable to nanostructure formation with additional depleting surface gates. Fabrication of nanostructures and study their noise properties are currently underway.

Acknowledgments

This work was supported by the Office of the Director of National Intelligence, Intelligence Advanced Research Projects Activity (IARPA), through the Army Research Office grant W911NF-12-1-0354. Y.A. is also supported by the United States Department of Defense. The views and conclusions contained in this document are those of the authors and should not be interpreted as representing the official policies, either expressly or implied, of the U.S. Government.

References

[1] J.R. Petta, A.C. Johnson, J.M. Taylor, E.A. Laird, A. Yacoby, M.D. Lukin, C. M. Marcus, M.P. Hanson, A.C. Gossard, Science 309 (2005) 2180.
[2] S. Foletti, H. Bluhm, D. Mahalu, V. Umansky, A. Yacoby, Nat. Phys. 5 (2009) 903–908.
[3] H. Bluhm, S. Foletti, I. Neder, M. Rudner, D. Mahalu, V. Umansky, A. Yacoby, Nat. Phys. 7 (2011) 109–113.
[4] M.D. Shulman, O.E. Dial, S.P. Harvey, H. Bluhm, V. Umansky, A. Yacoby, Science 336 (2012) 202–205.
[5] J. Medford, L. Cywinski, C. Barthel, C.M. Marcus, M.P. Hanson, A.C. Gossard, Phys. Rev. Lett. 108 (2012) 086802.
[6] J. Medford, J. Beil, J.M. Taylor, E.I. Rashba, H. Lu, A.C. Gossard, C.M. Marcus, Phys. Rev. Lett. 111 (2013) 050501.
[7] J. Medford, J. Beil, J.M. Taylor, S.D. Bartlett, A.C. Doherty, E.I. Rashba, D.P. DiVincenzo, H. Lu, A.C. Gossard, C.M. Marcus, Nat. Nanotechnol. 8 (2013) 654.
[8] A.P. Higginbotham, F. Kuemmeth, M.P. Hanson, A.C. Gossard, C.M. Marcus, Phys. Rev. Lett. 112 (2014) 026801.
[9] O.E. Dial, M.D. Shulman, S.P. Harvey, H. Bluhm, V. Umansky, A. Yacoby, Phys. Rev. Lett. 110 (2013) 146804.
[10] C. Buizert, F.H.L. Koppens, M. Pioro-Ladrière, P. Tranitz, I.T. Vink, S. Tarucha, W. Wegscheider, L.M.K. Vandersypen, Phys. Rev. Lett. 101 (2008) 226603.
[11] M. Pioro-Ladrière, J.H. Davies, A.R. Long, A.S. Sachrajda, L. Gaudreau, P. Zawadzki, J. Lapointe, J. Gupta, Z. Wasilewski, S. Studenikin, Phys. Rev. B 72 (2005) 115331.
[12] C. Kurdak, C.J. Chen, D.C. Tsui, S. Parihar, S. Lyon, Phys. Rev. B. 56 (1997) 15.
[13] Y. Li, C. Ren, P. Xiong, S. von Molnár, Y. Ohno, H. Ohno, Phys. Rev. Lett. 93 (2004) 246602.
[14] B.E. Kane, L.N. Pfeiffer, K.W. West, C.K. Harnett, Appl. Phys. Lett. 63 (1993) 2132.
[15] B.E. Kane, L.N. Pfeiffer, K.W. West, Appl. Phys. Lett. 67 (1995) 1262.
[16] B.E. Kane, G.R. Facer, A.S. Dzurak, N.E. Lumpkin, R.G. Clark, L.N. Pfeiffer, K. W. West, Appl. Phys. Lett. 72 (1998) 3506.
[17] R.H. Harrell, K.S. Pyshkin, M.Y. Simmons, D.A. Ritchie, C.J.B. Ford, G.A.C. Jones, M. Pepper, Appl. Phys. Lett. 74 (1999) 2328.
[18] O. Klochan, W.R. Clarke, R. Danneau, A.P. Micolich, L.H. Ho, A.R. Hamilton, K. Muraki, Y. Hirayama, Appl. Phys. Lett. 89 (2006) 092105.
[19] S. Sarkozy, K. Das Gupta, C. Siegert, A. Ghosh, M. Pepper, I. Farrer, H.E. Beere, D. A. Ritchie, G.A.C. Jones, Appl. Phys. Lett. 94 (2009) 172105.
[20] W.Y. Mak, K. Das Gupta, H.E. Beere, I. Farrer, F. Sfigakis, D.A. Ritchie, Appl. Phys. Lett. 97 (2010) 242107.
[21] W.Y. Mak, F. Sfigakis, K. Das Gupta, O. Klochan, H.E. Beere, I. Farrer, J.P. Griffiths, G.A.C. Jones, A.R. Hamilton, D.A. Ritchie, Appl. Phys. Lett. 102 (2013) 103507.
[22] A.M. See, O. Klochan, A.R. Hamilton, A.P. Micolich, M. Aagesen, P.M. Lindelof, Appl. Phys. Lett. 96 (2010) 112104.
[23] J.C.H. Chen, D.Q. Wang, O. Klochan, A.P. Micolich, K. Das Gupta, F. Sfigakis, D. A. Ritchie, D. Reuter, A.D. Wieck, A.R. Hamilton, Appl. Phys. Lett. 100 (2012) 052101.
[24] R.L. Willett, L.N. Pfeiffer, K.W. West, Appl. Phys. Lett. 89 (2006) 242107.
[25] R.L. Willett, M.J. Manfra, L.N. Pfeiffer, K.W. West, Appl. Phys. Lett. 91 (2007) 033510.

[26] T.M. Lu, D.R. Luhman, K. Lai, D.C. Tsui, L.N. Pfeiffer, K.W. West, Appl. Phys. Lett. 90 (2007) 112113.
[27] A.F. Croxall, B. Zheng, F. Sfigakis, K. Das Gupta, I. Farrer, C.A. Nicoll, H.E. Beere, D.A. Ritchie, Appl. Phys. Lett. 102 (2013) 082105.
[28] S. Sarkozy, K.D. Gupta, F. Sfigakis, I. Farrer, H.E. Beere, R. Harrell, D.A. Ritchie, G. A.C. Jones, Electrochem. Soc. Proc. 11 (2007) 75.
[29] J.H. Kim, D.H. Lim, G.M. Yang, J. Vac. Sci. Technol. B 16 (2) (1998) 558–560.
[30] E.H. Hwang, S. Das Sarma, Phys. Rev. B 77 (2008) 235437.
[32] A. Valeille, K. Muraki, Y. Hirayama, Appl. Phys. Lett. 92 (2008) 152106.
[33] NextNano3 simulator©, Walter Schottky Institute 1999–2008.
[34] D. Laroche, S. Das Sarma, G. Gervais, M.P. Lilly, J.L. Reno, Appl. Phys. Lett. 96 (2010) 1622112.
[35] D.J. Reilly, C.M. Marcus, M.P. Hanson, A.C. Gossard, Appl. Phys. Lett. 91 (2007) 162101.
[36] D.Q. Wang, J.C.H. Chen, O. Klocham, K. Das Gupta, D. Reuter, A.D. Wieck, D. A. Ritchie, A.R. Hamilton, Phys. Rev. B 87 (2013) 195313.
[37] P.T. Coleridge, Phys. Rev B 44 (1991) 3793.